NRC Research Press

ARTICLE

Previous growing season climate controls the occurrence of black spruce growth anomalies in boreal forests of Eastern Canada

Clémentine Ols, Annika Hofgaard, Yves Bergeron, and Igor Drobyshev

Abstract: To better understand climatic origins of annual tree-growth anomalies in boreal forests, we analysed 895 black spruce (*Picea mariana* (Mill.) B.S.P.) tree-growth series from 46 xeric sites situated along three latitudinal transects in Eastern Canada. We identified interannual (based on comparison with previous year growth) and multidecadal (based on the entire tree-ring width distribution) growth anomalies between 1901 and 2001 at site and transect levels. Growth anomalies occurred mainly at site level and seldom at larger spatial scales. Both positive interannual and multidecadal growth anomalies were strongly associated with below-average temperatures and above-average precipitation during the previous growing season (June$_{t-1}$ – August$_{t-1}$). The climatic signature of negative interannual and multidecadal growth anomalies was more complex and mainly associated with current-year climatic anomalies. Between the early and late 20th century, only negative multidecadal anomalies became more frequent. Our results highlight the role of previous growing season climate in controlling tree growth processes and suggest a positive association between climate warming and increases in the frequency of negative multidecadal growth anomalies. Projected climate change may further favour the occurrence of tree-growth anomalies and enhance the role of site conditions as modifiers of tree response to regional climate change.

Key words: ecological resilience, climate change, growth sensitivity, adaptive capacity, forest productivity.

Résumé : Nous avons étudié l'origine climatique des anomalies de croissance des forêts boréales en analysant 895 séries de croissance d'épinette noire (*Picea mariana* (Mill.) B.S.P.) provenant de 46 sites xériques repartis le long de trois transects latitudinaux dans l'Est Canadien. Nous avons identifié les anomalies de croissance interannuelles (comparaison à l'année précédente) et multi-décennales (comparaison à toutes les années) pour chaque site et transect de 1901 à 2001. Les anomalies de croissance apparaissent principalement à l'échelle du site mais rarement à de plus larges échelles géographiques. Les anomalies positives (interannuelles et multi-décennales) sont fortement associées à des températures basses et des précipitations fortes pendant la saison de croissance de l'année précédente. L'origine climatique des anomalies négatives (interannuelles et multi-décennales) est plus complexe et généralement associée à des anomalies climatiques de l'année en cours. Entre le début et la fin du XX^{e} siècle, seules les anomalies multi-décennales négatives sont devenues plus fréquentes. Nos résultats révèlent l'importance du climat de la saison de croissance précédente dans l'apparition d'anomalies de croissance et suggèrent un lien positif entre le réchauffement climatique et l'augmentation de la fréquence des anomalies multi-décennales négatives. L'augmentation prévue des températures dans les prochaines décennies pourrait davantage accroitre la fréquence des anomalies.

Mots-clés : résilience écologique, changement climatique, sensitivité de croissance, capacité d'adaptation, production forestière.

Introduction

Recent climate dynamics indicate an increase in global mean temperature and in the frequency and intensity of climate extremes (Intergovernmental Panel on Climate Change (IPCC) 2014). Trees have shown physiological limitations to cope with the rate of climate changes (Renwick and Rocca 2015), as evidenced by the occurrence of recent geographically widespread growth declines (Girardin et al. 2014) and drought-induced mortality (Allen et al. 2010). Effects of climate change on tree growth are most often assessed by correlating continuous time series of annual tree-rings data with climate variables (Fritts 1976). Among less common approaches is the use of discontinuous series such as binary time series of years of growth anomalies that also provide information on the effects of climate anomalies on tree-growth dynamics (Neuwirth et al. 2007). Nevertheless, the influence of climate extremes on tree growth and, particularly, on the occurrence of tree-growth anomalies is complex and still poorly understood. Existing studies suggest that, depending on their timing, duration, and intensity, climate extremes impact tree growth in different ways. For instance, unusually low precipitation during spring and summer has often been associated with reduced tree growth, whereas similar anomalies in autumn and winter rarely affect growth (Zeppel et al. 2014). Similarly, frost events prior to bud break usually do not impact growth, whereas frost events following bud break can damage newly formed needles or leaves and lead to a decreased growth during the remaining growing period (Sutinen et al. 2001). Moreover, due to temporal changes in tree sensitivity to climate, recurrent climate extremes during an individual tree's lifespan may trigger contrasting growth responses (Fritts 1976).

Received 23 October 2015. Accepted 5 March 2016.

C. Ols and Y. Bergeron. Institut de Recherche sur les Forêts, Université du Québec en Abitibi-Témiscamingue, 445 boul. de l'Université, Rouyn-Noranda, QC J9X 5E4, Canada.
A. Hofgaard. Norwegian Institute for Nature Research, P.O. Box 5685 Sluppen, NO-7485 Trondheim, Norway.
I. Drobyshev. Institut de Recherche sur les Forêts, Université du Québec en Abitibi-Témiscamingue, 445 boul. de l'Université, Rouyn-Noranda, QC J9X 5E4, Canada; Southern Swedish Forest Research Centre, Swedish University of Agricultural Sciences, P.O. Box 49, SE-230 53 Alnarp, Sweden.
Corresponding author: Clémentine Ols (email: clementine.ols@uqat.ca).

Despite the complexity of associations between climate extremes and growth anomalies, temporal changes in the frequency of growth anomalies may reflect occurrence of extreme weather conditions at regional scales (Fonti et al. 2010) and may also provide information on tree sensitivity and tree capacity to adapt to climate change, especially in well-drained sites where trees are more sensitive to changes in precipitation patterns (Fritts 1976). For example, narrow rings formed during droughts are generally characterized by higher proportions of latewood cells that increase tree "hydraulic safety" (Pothier et al. 1989). The plasticity of anatomical structure in tree rings may therefore represent an adaptation strategy to withstand soil water deficits (Bigler and Veblen 2009). On the other hand, more frequent negative growth anomalies may reflect an increase in the occurrence of drought conditions whereas more frequent positive growth anomalies may reflect trees' capacity to maintain high growth levels despite changes in mean climate and climate variability. The use of temporal changes in the frequency of growth anomalies as proxy for climate variability and (or) tree capacity to withstand such variability calls for a better understanding of associations between regional climate dynamics and growth anomalies.

Growth anomalies are commonly studied on annually resolved tree-ring series (Schweingruber et al. 1990). Anomalies observed in a large proportion of individual tree-growth series within the same site or region have been called pointer years (Schweingruber et al. 1990) and have been associated with large-scale climatic anomalies (Schultz et al. 2009), insect outbreaks (Boulanger et al. 2012), and volcanic eruptions (Gennaretti et al. 2014).

Boreal forests in Canada cover 55% of the land area and are dominated by black spruce (*Picea mariana* (Mill.) B.S.P.). Because of its ecological and economical importance, large geographical distribution, and sensitivity to climate, black spruce has been widely used to study climate–growth interactions (Hofgaard et al. 1999; Rossi et al. 2006). Growth declines have been reported to dominate across old-growth black spruce forests of North America (Girardin et al. 2012). These results suggest that the benefits of warmer temperatures such as a longer growing season may not necessarily counterbalance the moisture stress and respiration-associated carbon loss triggered by higher temperatures.

In Eastern Canada, seasonal temperatures have increased since the beginning of the 20th century (Hansen et al. 2010), whereas seasonal precipitations have shown inconsistent patterns (Wang et al. 2014). Warmer temperatures increase tree respiration, decrease trees' carbon stock, and shift carbon allocation from the stem to roots or foliage (Gifford and Evans 1981). Such changes in allocation patterns may favour the occurrence of growth anomalies. In the boreal forest of western Quebec, pointer years of black spruce have recently been associated with anomalies in spring and summer weather (Drobyshev et al. 2013). However, no studies have yet specifically investigated the spatiotemporal frequency and climatic origin of black spruce growth anomalies at synoptic (10 000 km^2) scales. In this paper, we analyze the (1) spatiotemporal patterns and (2) climatic origin of pointer years across province-wide climatic gradients in well-drained boreal forests in Quebec. We formulate three hypotheses: (*i*) pointer years occur synchronously across climatic gradients within boreal Quebec, (*ii*) pointers years are mainly associated with climatic anomalies during the growing season, and (*iii*) in the face of climate change, negative and positive pointer years have become more and less frequent, respectively.

Material and methods

Study area

We studied black spruce growth along three latitudinal transects in northern Quebec (Fig. 1). The western transect (hereafter, West) is characterised by low plains (200–350 m above sea level (a.s.l.)), whereas the central and eastern transects (hereafter, Central and East, respectively) are dominated by hills (400–800 m a.s.l.), which are particularly pronounced in the north. Dominant overlying bedrock deposits consist of peat along the West and of till along the Central and East (Ministère des Ressources naturelles du Québec 2013). The two main climatic gradients in the study area are a decreasing temperature gradient from south to north and an increasing summer precipitation gradient from west to east. July and January are the warmest and coldest months of the year, respectively (Table 1). The mean growing season length (1971–2000), starting 10 days after the mean daily temperature is above 5 °C and ending at fall frost, ranges from <100 days in northern parts to 110–120 days in southern parts of all transects (Agriculture and Agri-Food Canada 2014). The growing season starts in late April in the West and early May in the Central and East and ends in early October in all transects (Table 1). The whole study area receives a similar amount of precipitation between May and September, even if it rains substantially less along the West than along the Central and East over June to August (Fig. 1). Major snowfall periods occur in December and January in all transects, with additional important snowfall in March in the Central and East (Table 1). Due to these temperature and precipitation gradients, current fire cycles are shorter in the western part (about 95 years) than in the eastern part (up to 2000 years) of the study area (Ministère des Ressources naturelles du Québec 2013).

Site selection and sampling

We selected 14 to 17 sampling sites along each transect (Table 1; Fig. 1) using the 2007 Provincial Forest Inventory (Ministère des Ressources naturelles du Québec 2009). Most sites were situated in the spruce–moss forest bioclimatic domain; however, a few of the northernmost sites were located in the spruce – lichen domain (Fig. 1; Supplementary Table S1[1]). Selected sites consisted of unmanaged black spruce forests (>100 years old) on well-drained soils. We selected unmanaged forests to minimize anthropogenic impacts on growth patterns, old stands to allow the construction of long series, and sites on well-drained soils (xeric to mesoxeric) to maximize precipitation signal in tree-growth series and drought effects on tree growth.

At each site, we collected 3–16 cores from dominant healthy living trees (one core per tree) and 0–15 cookies from dead trees (one cookie per tree) (Supplementary Table S2[1]). We sampled cores and cookies as close as possible to the ground but above stem base deformities using an increment borer and chainsaw, respectively. The total number of samples per site ranged from 10 to 27 (Table 1; Supplementary Table S2[1]). Dead trees were sampled to extend series and accounted for 0%–100% (40% on average) of the sampled trees per site (Supplementary Table S2[1]). We attempted to restrict sampling of dead trees to snags of trees that were dominant when still alive. Ten pre-selected sites along the West burnt before sampling in 2013. As no trees had survived, sampling was adapted accordingly to only include recently dead but previously dominating trees (15 cookies per site; Supplementary Table S2[1]). We sampled trees during the summers of 2013 and 2014.

Sample preparation, crossdating, and measurements

Tree-growth samples were sanded, scanned, and measured with an accuracy of 0.01 mm using the CooRecorder program (Cybis Elektronik & Data AB 2015). Prior to analyses, we quality checked each tree-growth series. First, we visually and statistically crossdated tree-growth series at site level using the R package dplR (Bunn 2010) and the COFECHA program (Grissino-Mayer 2001). Following crossdating, we excluded tree-growth series presenting a low correlation ($r < 0.4$) with their respective site master (average of all series of a site except the focal series). We also excluded tree-growth

[1]Supplementary data are available with the article through the journal Web site at http://nrcresearchpress.com/doi/suppl/10.1139/cjfr-2015-0404.

Fig. 1. Location, bioclimatic domains (*a* and *b*), and climate (*c*) of the study area and study sites along the latitudinal West (black), Central (red), and East (blue) transects in northern Quebec. The median site latitude on each transect separates southern sites (circles) from northern sites (triangles). Mean temperature (°C) and precipitation (mm) along each transect are presented. Standard deviation for each climate variable is added in pale colors. Figure is provided in colour online.

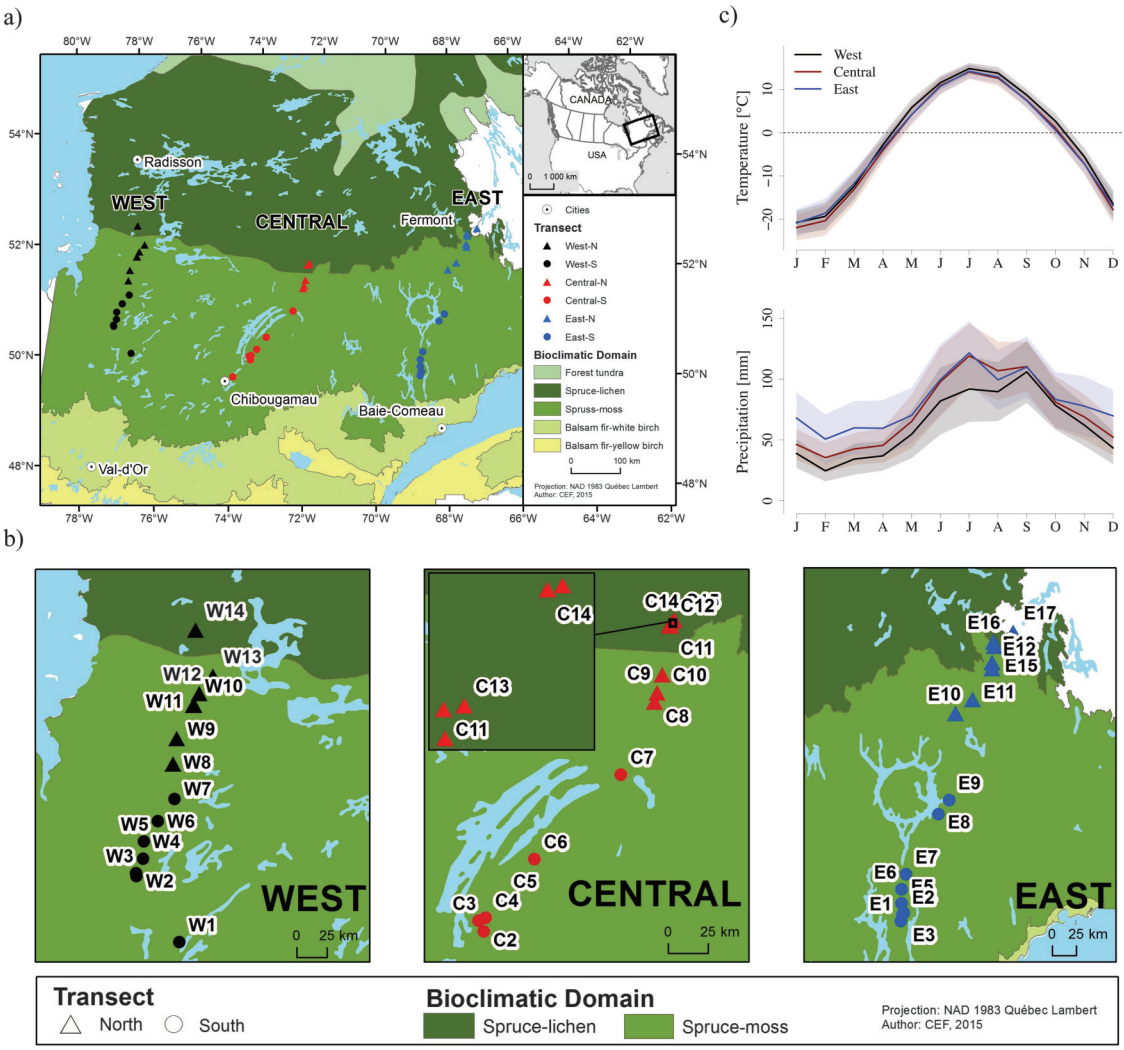

Table 1. Characteristics of transects.

	West	Central	East
Sampling			
Sites	14	15	17
Series per site (range)	10–22	19–25	12–27
Series per transect	183	342	370
Site series length (range in years)	120–302	140–312	136–301
Climate			
Latitude (WGS84)	(50.3N, 52.6N)	(50N, 52.2N)	(50.2N, 52.9N)
Longitude (WGS84)	(–77.7E, –77.1E)	(–74.1E, –72.1E)	(–68.8E, –67.1E)
Growing season	late April–early October	early May–early October	early May–early October
Growing season (days)	<100–120	<100–120	<100–120
Warmest month (minimum, maximum; °C)	July (11, 18)	July (10, 19)	July (10, 19)
Coldest month (minimum, maximum; °C)	January (–29, –14)	January (–30, –14)	January (–29, –13)
Months with the most snow	December–January	December–January–March	December–January–March
Months with the most rain	September	July (September)	July (September)

Note: Climate data represent variability in site-level climate along each transect.

series presenting any growth reduction longer than 5 years that synchronized with years of known spruce budworm (*Choristoneura fumiferana* (Clem.)) outbreaks (Boulanger and Arseneault 2004). Out of 1380 tree-growth series, 895 passed the quality check and were used in the analyses, with 183, 342, and 370 individual tree-growth series along the West, Central, and East, respectively (Table 1; Supplementary Table S2[1]). Quality checked tree-growth series were then log transformed, detrended using a 32 year spline, and

prewhitened (Cook and Peters 1997). This standardisation procedure kept high-frequency variations in growth, mainly linked to climate variability, while removing low-frequency variations commonly related to biological or stand-level effects. As a result, the standardisation increased correlation between tree-growth series and climate. Finally, we built raw and detrended site series, calculated as the biweighted robust mean of all raw or detrended series from a site (Supplementary Table S2[1]). Site series lengths ranged from 120 to 312 years (Table 1; Supplementary Table S2[1]). Most raw site series presented a signal-to-noise ratio greater than 2 and an expressed population signal greater than 0.6. Both indicators generally increased after detrending (Supplementary Table S2[1]).

Identification of pointer years

Pointer years are commonly defined as growth anomalies appearing synchronously in several individual tree-growth series within a specific geographical region or site (Fritts 1976). The identification of pointer years can vary substantially depending on the time frame within which anomalies are defined (Bijak 2008). In this study, we concomitantly considered two definitions of pointer years previously used in the literature. First, we considered pointer years as interannual growth anomalies, also known as a pointer interval (Schweingruber et al. 1990). We termed these as year-to-year (YTY) pointer years. YTY pointer years were defined as years in which at least 75% of the trees within a site recorded a 10% increase or decrease in ring width compared with the previous year (Mérian 2012). Second, we considered pointer years as multidecadal growth anomalies, i.e., years in which tree-ring width fell outside the central 90% of the ring width distribution of a tree. We termed these as quantile (QTL) pointer years. QTL pointer years were defined as years in which at least 20% of the trees within a site exhibited a growth in the upper and lower 5% quantiles of the distribution (Drobyshev et al. 2013). The two identification methods differ in initial inputs (raw series for YTY pointer years and detrended series for QTL pointer years) and in the temporal scale at which anomalies are defined (short-term variability in YTY pointer years and long-term variability, i.e., over the entire lifespan of an individual tree, in QTL pointer years).

We identified positive and negative pointer years at site level when site series included at least 10 individual tree series between 1901 and 2001. All site series presented a sample depth of 10 over the entire study period except six series in the West that had a replication of only 10, namely 1900–1950, 1920–1974, 1900–1973, 1900–1988, 1900–1972, and 1918–2001. Lastly, we identified years in which at least 50% of the site series within a transect recorded a pointer year of identical sign (positive or negative), hereafter named main pointer years.

Ordination of pointer years' occurrence at site level

Between 1901 and 2001, we coded pointer years as 1 and all other years as 0 and built site-specific binary time series for each of the four types of pointer years (positive or negative and YTY or QTL). Years with a sample depth less than 10 trees were coded as NA. We evaluated between-site similarity in the occurrence of pointer years by nonmetric multidimensional scaling using the R package vegan (Oksanen et al. 2015). This ordination method condenses a set of multiple time series into a set of two or three principal components (dimensions) to facilitate the visual interpretation of the results. The ordination was performed separately for each type of pointer year using Euclidean distances between binary time series. We ran the ordination at a two-dimension level with a limit of 150 random iterations. However, stable results were always found after a maximum of 10 iterations.

Synchronicity of pointer years along and across transects

To account for possible random effects on synchronicity, we tested differences between observed and expected frequencies of synchronous pointer years along and across transects between 1901 and 2001 using a χ^2 test. Considering within-transect synchronicity, we calculated transect-specific ratios of observed vs. expected number of years with zero to N sites synchronously presenting a pointer year. N was the highest observed number of sites synchronously recording a pointer year. Similarly, to evaluate synchronicity levels across transects, we calculated ratios of observed vs. expected number of years with zero to three transects synchronously presenting a main pointer year (cf. identification of pointer years). To comply with requirements of the χ^2 test, we aggregated data into classes with expected frequency greater than five.

Climate data

Climate data from meteorological stations in Quebec are too scarce to perform accurate and reliable climate-growth analyses at large geographical scales. We, therefore, used climate data from the 0.5° × 0.5° CRU TS 3.22 global dataset (Harris et al. 2014). Site-specific climate data were extracted using 0.5° × 0.5° grid cells, each site location defining the centre of a climatic grid cell. Prior to analyses, we verified the quality of the extrapolated grid data by comparing them with climate data from 11 meteorological stations in Quebec (Environment Canada 2014) that had not been used in the construction of the CRU dataset (Supplementary Table S3[1]). We averaged station data at the transect level and compared them with the mean of all site-specific 0.5° × 0.5° grid cells data along each transect between 1936 and 2004, the longest common period between both types of climate data. Grid data correlated well ($r > 0.97$) with station data, preserving climate variability within and between transects, i.e., north–south temperature and west–east precipitation gradients (data not shown). The extrapolated grid data were, therefore, selected as climate input for all further analyses. The mean climatic characteristics of each transect between 1901 and 2001 are presented in Table 1. In addition to temperature and precipitation, we extracted monthly North Atlantic Oscillation and Arctic Oscillation indices from the Climate Prediction Center database (National Oceanic and Atmospheric Administration (NOAA) 2014) between 1950 and 2001.

Associations between pointer years and climate

We studied associations between the occurrence of pointer years and climatic anomalies at site level through superposed epoch analyses using the R package dplR (Bunn 2010). These analyses evaluate whether the mean values of climate variables during pointer years significantly differ from their mean values during normal years. Climate variables included monthly mean, maximum, and minimum temperatures, total precipitation, and the two monthly oscillation indices. We performed superposed epoch analyses for each of the four types of pointer years (positive or negative and YTY or QTL). We ran analyses on the longest common period between climatic records and site-specific binary time series, i.e., 1901–2001 for temperature and precipitation and 1950–2001 for the two oscillation indices. Analyses included months from previous May (May_{t-1}) to current August (August_t).

In addition, we studied climate–growth interactions along each transect by investigating correlations and response functions between detrended transect series (average of all detrended site series along a transect) and the above-mentioned climate variables. Analyses were performed using the R package bootRes (Zang and Biondi 2013). All correlations and response functions were tested for 95% confidence intervals using 1000 bootstrap samples.

Temporal changes in the frequency of pointer years

We studied changes in the frequency of pointer years between 1901 and 2001 by dividing the study period into three subperiods, each approximately 30 years long (1901–1935, 1936–1970, and 1971–2001). This temporal division, based on the definition of climate by the World Meteorological Organization (WMO) (2015), assumes a 30-year block–stationary climate (Visser and Petersen 2012). We partitioned our study area into six regions by dividing

each transect into a northern and southern region (Fig. 1; Supplementary Table S1[1]). The north–south delimitation along each transect was defined by the median latitude of all sites.

We identified changes in the frequency of pointer years between the first (1901–1935) and last (1971–2001) subperiods using generalized linear models with binomial distribution (Crawley 2005). Models were run at a regional level. For each region, we tested the significance of temporal changes in pointer year frequencies, aggregating data from all site-specific binary time series within that region. In case of over-dispersion in the residuals, we refitted the models using quasibinomial distribution and performed a Pearson's χ^2 test to test for significance in differences following this readjustment (Crawley 2005). All χ^2 tests were significant at $p < 0.05$.

Results

Among-site similarities in occurrence of pointer years

Regardless of the type of pointer year, the ordination revealed strong longitudinal and latitudinal patterns in the occurrence of pointer years, particularly for negative pointer years (Fig. 2). The aggregation level of ordination was generally low for all types of pointer years, except for QTL positive pointer years in which sites were strongly aggregated around the origin of the ordination (Fig. 2). For all types of pointer years, the West was the most geographically defined group, although some overlap occurred between the Central and East, especially during positive pointer years.

Spatial scale of pointer year occurrence

Both YTY and QTL pointer years mainly occurred at site level and more rarely at larger scales, as underlined by the few main pointer years (2 to 7) identified on each transect (Fig. 3). This low synchronicity along all transects was, nevertheless, significantly higher than what would be expected by a random process (Table 2).

Only 3 out of 18 YTY main pointer years (1927, 1959, and 1974) were recorded simultaneously on two transects, whereas no synchronous QTL main pointer year occurred across transects (Fig. 3). This level of synchronicity across transects was significantly lower than would be expected by a random process (Table 2).

The occurrence of main pointer years was temporally irregular and transect specific (Fig. 3). QTL main pointer years did not reveal clear temporal patterns in any of the transects, and YTY main pointer years only occurred between 1920 and 1960 in the East, precisely when they ceased occurring in the West. Along the Central, YTY main pointer years only occurred between 1960 and 1980, except 1927. Regardless of the pointer year type, the number of positive and negative main pointer years was identical in the West and East. YTY main pointer years were more numerous than QTL main pointer years on all transects (Fig. 3).

Spatial frequency of main pointer years

The spatial distribution of sites recording either YTY or QTL main pointer years varied over the study period along each transect (Fig. 4). Nevertheless, a number of main pointer years predominantly occurred at southern or northern sites, e.g., YTY 1924 in the East and YTY 1927 in the Central. Along the West, both YTY and QTL main pointer years tended to occur more often in the north. Along the Central, all main pointer years before 1960 mostly occurred at northern sites, their occurrence extending southward thereafter but disappearing from the central part of the transect (C8–C12). Along the East, main pointer years (both YTY and QTL) in the late 1950s had a dominant northern occurrence.

The latitudinal range of sites recording YTY main pointer years was larger than those recording QTL main pointer years, e.g., 1913 in the West and 1943 in the East (Fig. 4). All or almost all main pointer years occurred at some sites (W10–W12, C7, and E5), whereas, at other sites, only a few were observed (C1 and E1) (Fig. 4).

Fig. 2. Nonmetric multidimensional scaling of positive and negative year to year (YTY) and quantile (QTL) pointer year occurrence at site level between1901 and 2001. West (W), Central (C), and East (E) sites are plotted in black, red, and blue, respectively. Latitude and longitude (arrows) significantly explained each ordination ($p < 0.01$). *s* values give the stress of the ordination, and values between 0.1 and 0.2 usually provide a good representation of multidimensional between-site distances. Figure is provided in colour online.

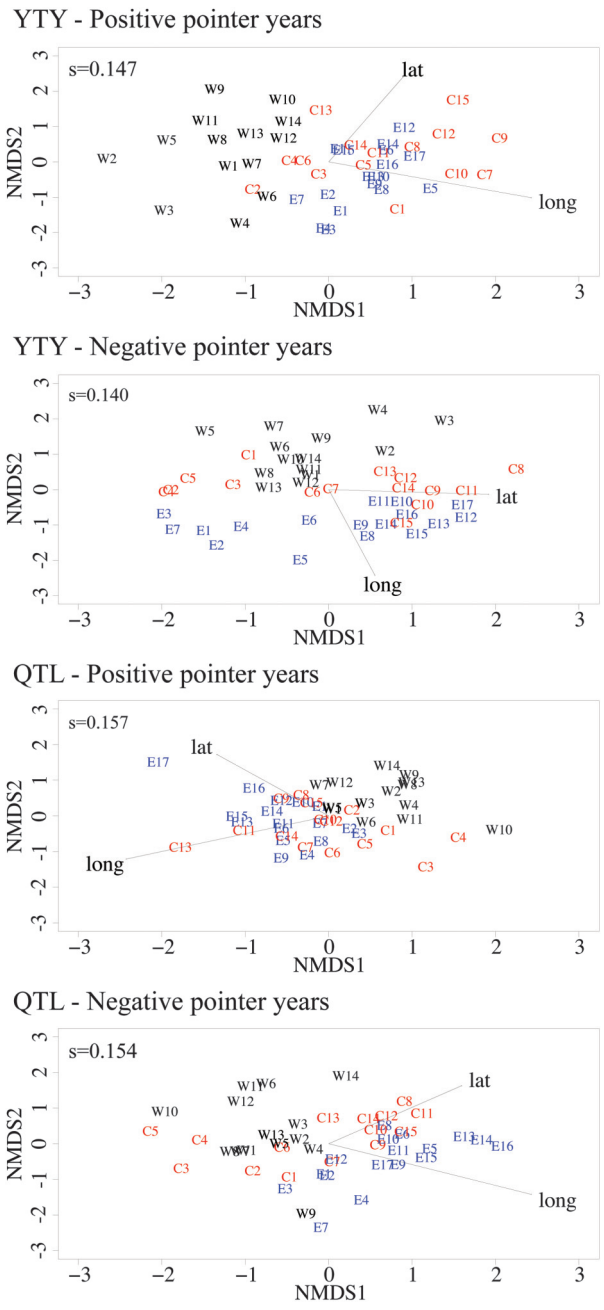

Climatic origin of pointer years

Regardless of their type, positive pointer years were mainly associated with climatic anomalies during the previous growing season, whereas negative pointer years were mainly associated with current year climatic anomalies. Significant associations observed with mean, maximum, and minimum temperatures were mostly similar (Supplementary Fig. S5[1]). Few significant associations with monthly oscillation indices were found, and these were site specific (Supplementary Fig. S5[1]).

Fig. 3. Transect-level frequency and occurrence of pointer years for 1901–2001. Results for year to year (YTY) and quantile (QTL) pointer years are respectively presented in the upper and lower sections of the figures. Left *Y* axes show proportion of sites (%) recording a pointer year for each calendar year. Right *Y* axes show the number of sites included in the analyses through time (horizontal lines). Positive and negative pointer years are plotted in black and grey, respectively. Calendar years' markers are given for main pointer years, i.e., years when more than 50% of the sites along a transect record the same pointer year.

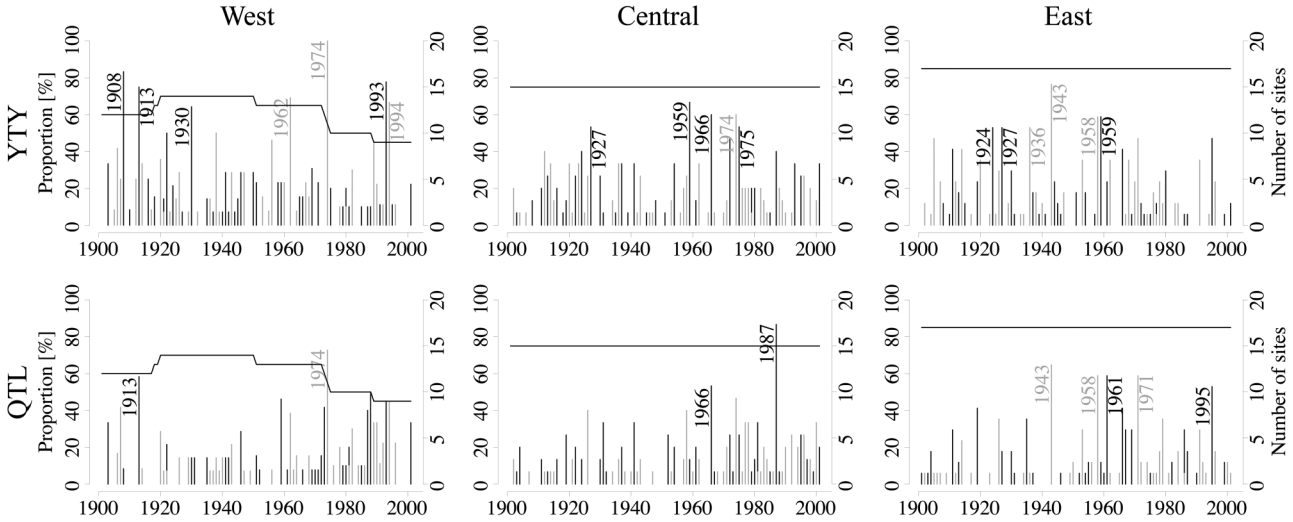

Table 2. Pointer years' synchronicity along and across transects.

	χ^2	df	*p* value
YTY pointer years			
Along transects			
West	33.0	4	**<0.001**
Central	44.4	4	**<0.001**
East	40.7	4	**<0.001**
Across transects	0.2	1	0.7
QTL pointer years			
Along transects			
West	9.9	3	**0.02**
Central	6.6	3	0.09
East	21.1	4	**<0.001**
Across transects	0.04	1	0.8

Note: The table presents results of contingency analyses for YTY and QTL pointer years, respectively; only collapsed χ^2 statistics are presented in the table. Significant *p* values ($p < 0.05$) are in bold. YTY, year to year; QTL, quantile.

Positive pointer years

There was a strong and spatially consistent association between both positive YTY and QTL pointer years and below-average previous growing season mean temperatures (June$_{t-1}$ through August$_{t-1}$) (Fig. 5). This overall strong association was also highlighted by relatively high correlation and response function coefficients (Supplementary Table S4[1]). However, some differences between the climatic origin of YTY and QTL pointer years were evident. For instance, the association between positive pointer years and below-average August$_{t-1}$ temperature was only significant for YTY pointer years in the Central and West and for QTL pointer years in the East and West. Positive YTY pointer years were also associated with below-average temperatures in May$_{t-1}$ and December$_{t-1}$ in the East, and positive QTL pointer years were associated with below-average temperatures in October$_{t-1}$ through November$_{t-1}$ in the West and Central.

Significant associations between maximum temperature anomalies and positive pointer years (both YTY and QTL) were mostly comparable with those observed for mean temperature. However, associations observed with below-average mean temperature in November$_{t-1}$ and December$_{t-1}$ were no longer observed with maximum temperature. In addition, associations between QTL pointer years and above-average spring maximum temperature (April$_t$ – June$_t$), which were not observed for mean temperature, emerged in the Central.

Associations between positive pointer years and precipitation were few but mainly linked to above-average previous growing season anomalies. Positive YTY pointer years were associated with higher May$_{t-1}$ – June$_{t-1}$ precipitation, and positive QTL pointer years were linked to anomalously high July$_{t-1}$ – August$_{t-1}$ precipitation (Fig. 5).

Negative pointer years

Significant associations between the occurrence of negative pointer years and climatic anomalies were less numerous compared with the occurrence of positive pointer years and climatic anomalies (Fig. 5).

Both negative YTY and QTL pointer years were associated with below-average January$_t$ mean temperature in all transects. A strong association between negative YTY pointer years and below-average April$_t$ temperatures was found in the West.

Significant associations between maximum temperature anomalies and negative pointer years (both YTY and QTL) were largely comparable with those observed for mean temperature. However, we noticed that associations with below-average January$_t$ mean temperature in the Central and East were no longer observed for the maximum temperature. In addition, significant associations with below-average April$_t$ maximum temperatures were more numerous than for mean temperature.

Significant associations with precipitation were rare and very site specific (Fig. 5). However, both types of negative pointer years were significantly associated with above-average May$_t$ precipitation (Fig. 5).

Temporal changes in the frequency of pointer years

We detected few significant changes in the frequency of YTY and QTL pointer years between the early and late 20th century. The frequency of positive pointer years of both types remained largely the same between these two periods, except in the West. There, the frequency of positive YTY pointer years increased in the southern region, whereas the frequency of positive QTL pointer years decreased in the northern region (Fig. 6).

Fig. 4. Spatial frequency of main pointer years along their respective transect (see Fig. 3 for identified main pointer years). Filled squares show site-level occurrence of transect-specific main pointer years. Negative and positive main pointer years are plotted in blue and red, respectively. Light and dark colors are used for year to year (YTY) and quantile (QTL) main pointer years, respectively. An "x" stands for years when pointer year identification was not conceivable (i.e., when sites series were based on less than 10 trees). Panels are aligned using the median latitude of each transect (thick, black horizontal line), representing the limit between southern and northern sites (West (W), 51.4°; Central (C), 51.5°; East (E), 51.3°). Figure is provided in colour online.

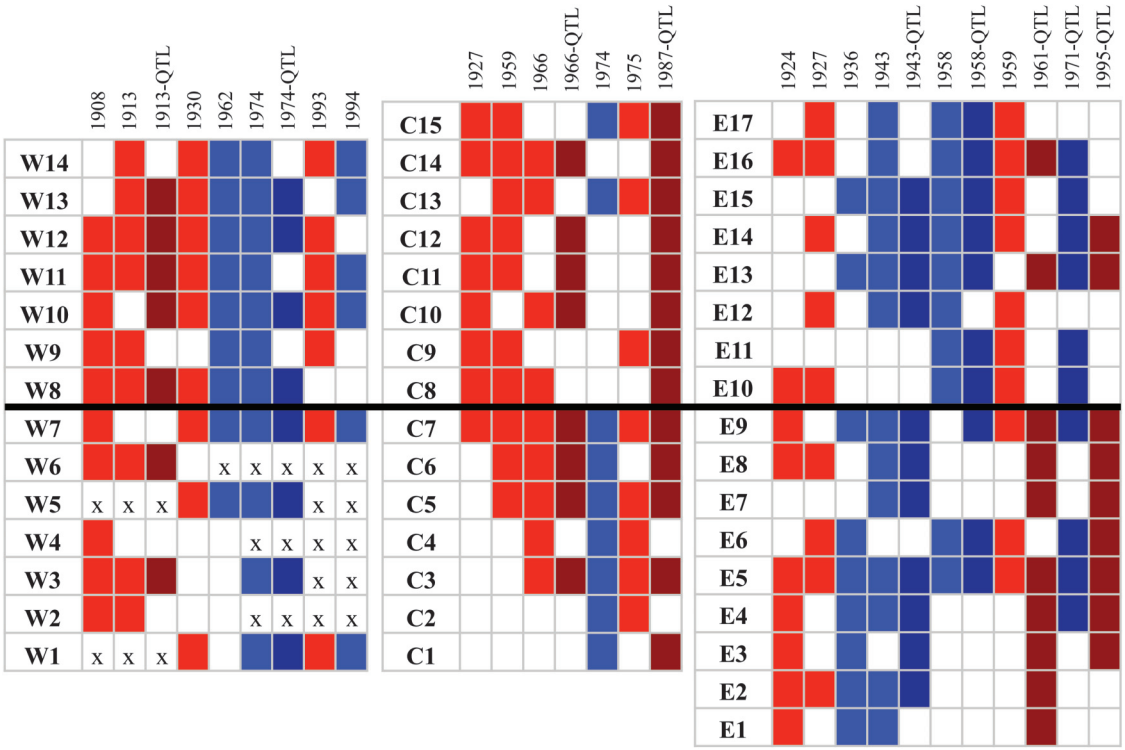

Negative QTL pointer years became significantly more frequent in all six regions between the early and late 20th century, whereas the frequency of negative YTY pointer years did not change, except in the southern region of the West, where it increased (Fig. 6).

Discussion

Spatial synchronicity of pointer years

Few pointer years synchronized across boreal Quebec, suggesting that, even if common climatic forcing causing extreme tree growth occurs, these events are rare, particularly along longitudinal gradients. This suggests that climatic forcing leading to the occurrence of synchronous growth events such as pointer years or frost rings (Plasse et al. 2015) occur more easily along latitudinal climatic gradients in our study area. Longitudinal climatic gradients in boreal Quebec, triggering differences in climate-growth relationships in black spruce (Nicault et al. 2014), appear to prevent the formation of synchronous pointer years at large scales. Pointer years occurring simultaneously over the entire study area would involve large-scale climatic and biotic events such as volcanic eruptions (Gennaretti et al. 2014), anomalies in atmospheric circulation patterns (Schultz et al. 2009), and (or) region-wide synchronous insect outbreaks (Boulanger et al. 2012). However, our data did not suggest occurrence of such events during the 20th century.

Climatic origin of pointer years

Positive pointer years in boreal Quebec, despite their site-specific occurrence, originated from similar site-level climatic anomalies during the previous growing season. We hypothesize that low temperature and high precipitation anomalies during the previous growing season increase carbon accumulation before dormancy by lowering climatic stress, e.g., heat and water limitations, which results in growth-promoting higher carbon stocks the following growing season. Indeed, a recent study on black spruce growth across the entire boreal Canada has shown that water limitation and heat stress negatively affected carbon assimilation in black spruce the year preceding tree-ring formation and decreased growth during the subsequent growing season (Girardin et al. 2015). A positive effect of moist previous summers on black spruce growth during the subsequent growing season has also been previously reported for western Quebec (Hofgaard et al. 1999).

Negative pointer years of both types were not associated to any particular climatic conditions, suggesting that negative pointer years might arise from complex and temporally inconsistent combinations of climatic anomalies (Schultz et al. 2009). For example, repeated frost events during June and July, a period with high cambium activity (Rossi et al. 2006), have been shown to disturb growth and lead to the formation of negative pointer years (Plasse et al. 2015). The lack of consistent climatic signature in the occurrence of negative pointer years might also suggest that their appearance is strongly modulated by site-level factors (Neuwirth et al. 2004), e.g., topography (Desplanque et al. 1999) and (or) ground vegetation (Plasse et al. 2015).

Temporal changes in the frequency of pointer years

The large-scale increase in the frequency of negative QTL pointer years between the early and late 20th century echoes recent growth declines observed in boreal forests of North America (Girardin et al. 2014, 2015) and might, similar to reported growth declines, reflect negative effects of climate warming, e.g., heat stress, on multidecadal growth patterns (Girardin et al. 2015). The observed higher frequency of negative QTL pointer years does not appear to be linked to a decrease in water availability, as no significant changes in regional precipitation patterns occurred in the study area during the 20th century (Wang et al. 2014).

Fig. 5. Significant associations between the occurrence of pointer years and monthly temperature (T_{mean} and T_{max}) and total precipitation (1901–2001) at site level, as revealed by superposed epoch analyses. Analyses were run from previous May (May_{t-1}) to current August ($August_t$) and for positive (upper section) and negative (lower section) pointer years. Empty and filled circles represent significant associations found for year to year (YTY) and quantile (QTL) pointer years, respectively. Filled circles with a black outline are sites at which associations were significant for both YTY and QTL pointer years. Blue and red circles stand for significant association with below- and above-average climates, respectively. Maps of the study area are only plotted when three or more sites along the same transect presented a significant association ($p < 0.05$) to a specific monthly climate variable. Figure is provided in colour online.

Fig. 6. Changes in the frequency of pointer years between the early and late 20th century. Changes in the frequency of pointer years between the first (1901–1935) and last (1971–2001) subperiods were identified for each region using generalized linear models with either a binomial distribution or quasibinomial distribution, according to overdispersion. Blue "–" and red "+" indicate significant ($p < 0.05$) decreases and increases in the frequency of pointer years, respectively, and white "0" denote nonsignificant changes. W, C, E, N, and S stand for West, Central, East, North, and South, respectively. YTY, year to year; QTL, quantile. Figure is provided in colour online.

The temporally stable frequency of YTY pointer years (both positive and negative) between the early and late 20th century indicates that black spruce interannual growth variations, contrary to multidecadal growth variations, do not appear to be affected by climate change. This contradicts the fact that climate-change related phenomena such as the decrease in Arctic sea ice cover have been reported to significantly co-vary with interannual growth dynamics of black spruce in eastern North America (Girardin et al. 2014).

Growth anomalies as signs of tree growth vulnerability to climate change

The observed large-scale increase in the frequency of negative QTL pointer years between the early and late 20th century could reflect an increasing incapacity of trees to maintain stable above-ground growth in the face of warming temperatures. Such an increase might also point toward higher carbon allocation to roots to improve access to water and nutrients (Gifford and Evans 1981; Lapenis et al. 2013) during warmer growing conditions. A continuous increase in maximum tree ring density has been recently reported in eastern North America (Mannshardt et al. 2012). These observations, along with the observed increase in the frequency of negative QTL pointer years, imply that trees more often produce dense and narrow rings characterized by higher proportions of latewood cells. Because such cells increase hydraulic capacity (Pothier et al. 1989), more frequent negative pointer years could indicate a mitigation mechanism against heat stress and decreased water availability. Future studies need to investigate synergies between below- and above-ground growth dynamics of adult black spruces, e.g., to test whether declines in stem growth synchronize with increased root growth.

Conclusion

Growth anomalies seldom synchronized across sites, highlighting the site-specific occurrence of extreme growth events in black spruce forests of boreal Quebec. Despite their site-specific occurrence, positive growth anomalies were mainly triggered by climatic anomalies during the previous growing season. The lack of coherent climatic signature for negative growth anomalies suggested that their origin was more complex and modulated to a higher degree by nonclimatic factors, e.g., site-level factors, compared with positive growth anomalies. Our results call for further analyses on the role of site conditions (altitude, topography) and stand characteristics (tree age and density) in modulating tree responses to climate change.

Within the time frame of their definition, pointer years can bring important information on past climate–growth interactions. Because the time frame used to define growth anomaly strongly affects the outcome of pointer year identification and subsequent analyses, we generally advocate for the use of both short- and long-term time frames for more comprehensive and objective analyses.

Acknowledgements

This study was financed by the Natural Sciences and Engineering Research Council of Canada (NSERC) through the project "Natural disturbances, forest resilience and forest management: the study case of the Northern Limit for timber allocation in Quebec in a climate change context", by the Nordic Forest Research Cooperation Committee (SNS) through the network project entitled "Understanding the impacts of future climate change on boreal forests of Northern Europe and Eastern Canada" (grant No. 12262), and by support from Norwegian Institute for Nature Research's (NINA) core funding from the Research Council of Norway (project 160022/F40). We acknowledge Sylvain Larouche and Simon Paradis for their precious help during fieldwork and thank Jeanne Portier for providing us with additional tree-ring material. We also thank Xiao Jing Guo from the Canadian Forest Service for statistical support and Linda Shiffrin for language and grammar checking. Finally, we thank the two anonymous reviewers for comments and improvements on an earlier version of the paper.

References

Agriculture and Agri-Food Canada. 2014. Length of growing season in Quebec. Available from http://www.agr.gc.ca/eng/science-and-innovation/agricultural-practices/climate/future-outlook/climate-change-scenarios/length-of-growing-season-in-quebec/?id=1363104198111 [accessed 7 May 2015].

Allen, C.D., Macalady, A.K., Chenchouni, H., Bachelet, D., McDowell, N., Vennetier, M., Kitzberger, T., Rigling, A., Breshears, D.D., Hogg, E.H., Gonzalez, P., Fensham, R., Zhang, Z., Castro, J., Demidova, N., Lim, J.H., Allard, G., Running, S.W., Semerci, A., and Cobb, N. 2010. A global overview of drought and heat-induced tree mortality reveals emerging climate change risks for forests. For. Ecol. Manage. **259**(4): 660–684. doi:10.1016/j.foreco.2009.09.001.

Bigler, C., and Veblen, T.T. 2009. Increased early growth rates decrease longevities of conifers in subalpine forests. Oikos, **118**(8): 1130–1138. doi:10.1111/j.1600-0706.2009.17592.x.

Bijak, S. 2008. Various factors influencing the pointer year analysis. Tree Rings Archaeol. Climatol. Ecol **6**: 77–82.

Boulanger, Y., and Arseneault, D. 2004. Spruce budworm outbreaks in eastern Quebec over the last 450 years. Can. J. For. Res. **34**(5): 1035–1043. doi:10.1139/X03-269.

Boulanger, Y., Arseneault, D., Morin, H., Jardon, Y., Bertrand, P., and Dagneau, C. 2012. Dendrochronological reconstruction of spruce budworm (*Choristoneura fumiferana*) outbreaks in southern Quebec for the last 400 years. Can. J. For. Res. **42**(7): 1264–1276. doi:10.1139/x2012-069.

Bunn, A.G. 2010. Statistical and visual crossdating in R using the dplR library. Dendrochronologia, **28**: 251–258. doi:10.1016/j.dendro.2009.12.001.

Cook, E.R., and Peters, K. 1997. Calculating unbiased tree-ring indices for the study of climatic and environmental change. The Holocene, **7**(3): 361–370. doi:10.1177/095968369700700314.

Crawley, M.J. 2005. Count data. *In* Statistics: an introduction using R. John Wiley & Sons, Inc. pp. 227–245. doi:10.1002/9781119941750.ch13.

Cybis Elektronik & Data AB. 2015. CooRecorder. Available from http://www.cybis.se/forfun/dendro/index.htm.

Desplanque, C., Rolland, C., and Schweingruber, F.H. 1999. Influence of species and abiotic factors on extreme tree ring modulation: *Picea abies* and *Abies alba* in Tarentaise and Maurienne (French Alps). Trees, **13**: 218–227. doi:10.1007/s004680050236.

Drobyshev, I., Gewehr, S., Berninger, F., Bergeron, Y., and McGlone, M. 2013. Species specific growth responses of black spruce and trembling aspen may enhance resilience of boreal forest to climate change. J. Ecol. **101**(1): 231–242. doi:10.1111/1365-2745.12007.

Environment Canada. 2014. Climate historic data. Available from http://climate.weather.gc.ca/advanceSearch/searchHistoricData_e.html [accessed 10 October 2014].

Fonti, P., von Arx, G., García-González, I., Eilmann, B., Sass-Klaassen, U., Gärtner, H., and Eckstein, D. 2010. Studying global change through investigation of the plastic responses of xylem anatomy in tree rings. New Phytol. **185**(1): 42–53. doi:10.1111/j.1469-8137.2009.03030.x. PMID:19780986.

Fritts, H.C. 1976. Tree rings and climate. Academic Press, London.

Gennaretti, F., Arseneault, D., Nicault, A., Perreault, L., and Bégin, Y. 2014. Volcano-induced regime shifts in millennial tree-ring chronologies from northeastern North America. Proc. Natl. Acad. Sci. U. S. A. **111**(28): 10077–10082. doi:10.1073/pnas.1324220111. PMID:24982132.

Gifford, R.M., and Evans, L.T. 1981. Photosynthesis, carbon partitioning, and yield. Annu. Rev. Plant Physiol. **32**: 485–509. doi:10.1146/annurev.pp.32.060181.002413.

Girardin, M.P., Guo, X.J., Bernier, P.Y., Raulier, F., and Gauthier, S. 2012. Changes in growth of pristine boreal North American forests from 1950 to 2005 driven by landscape demographics and species traits. Biogeosciences, **9**: 2523–2536. doi:10.5194/bgd-9-2523-2012.

Girardin, M.P., Guo, X.J., De, Jong, R., Kinnard, C., Bernier, P., and Raulier, F. 2014. Unusual forest growth decline in boreal North America covaries with the retreat of Arctic sea ice. Glob. Chang. Biol. **20**(3): 851–866. doi:10.1111/gcb.12400. PMID:24115302.

Girardin, M.P., Hogg, E.H., Bernier, P.Y., Kurz, W.A., Guo, X.J., and Cyr, G. 2015. Negative impacts of high temperatures on growth of black spruce forests intensify with the anticipated climate warming. Global Change Biol. **22**(2): 627–643. doi:10.1111/gcb.13072.

Grissino-Mayer, H.D. 2001. Evaluating crossdating accuracy: a manual and tutorial for the computer program COFECHA. The University of Arizona Campus Repository, Tree-Ring Research, **57**(2): 205–221.

Hansen, J., Ruedy, R., Sato, M., and Lo, K. 2010. Global surface temperature change. Rev. Geophys. **48**(4). doi:10.1029/2010rg000345.

Harris, I., Jones, P.D., Osborn, T.J., and Lister, D.H. 2014. Updated high-resolution grids of monthly climatic observations — the CRU TS3.10 dataset. Int. J. Climatol. **34**(3): 623–642. doi:10.1002/joc.3711.

Hofgaard, A., Tardif, J.C., and Bergeron, Y. 1999. Dendroclimatic response of *Picea mariana* and *Pinus banksiana* along a latitudinal gradient in the eastern Canadian boreal forest. Can. J. For. Res. **29**(9): 1333–1346. doi:10.1139/x99-073.

Intergovernmental Panel on Climate Change (IPCC). 2014. IPCC fifth assessment report climate change 2014. synthesis report — summary for policymakers. pp. 1–35.

Lapenis, A.G., Lawrence, G.B., Heim, A., Zheng, C., and Shortle, W. 2013. Climate warming shifts carbon allocation from stemwood to roots in calcium-depleted spruce forests. Glob. Biogeochem. Cycles, **27**(1): 101–107. doi:10.1029/2011gb004268.

Mannshardt, E., Craigmile, P.F., and Tingley, M.P. 2012. Statistical modeling of extreme value behavior in North American tree-ring density series. Clim. Chang. **117**(4): 843–858. doi:10.1007/s10584-012-0575-5.

Mérian, P. 2012. POINTER et DENDRO: deux applications sous R pour l'analyse de la re′ponse des arbres au climat par approche dendroe′cologique. Rev. for. fr. **6**: 789–798.

Ministère des Ressources naturelles du Québec. 2009. Norme d'inventaire écodendrométrique nordique.

Ministère des Ressources naturelles du Québec. 2013. Rapport du Comité scientifique chargé d'examiner la limite nordique des forêts attribuables.

Neuwirth, B., Esper, J., Schweingruber, F.H., and Winiger, M. 2004. Site ecological differences to the climatic forcing of spruce pointer years from the Lötschental, Switzerland. Dendrochronologia, **21**(2): 69–78. doi:10.1078/1125-7865-00040.

Neuwirth, B., Schweingruber, F.H., and Winiger, M. 2007. Spatial patterns of central European pointer years from 1901 to 1971. Dendrochronologia, **24**(2–3): 79–89. doi:10.1016/j.dendro.2006.05.004.

Nicault, A., Boucher, E., Tapsoba, D., Arseneault, D., Berninger, F., Bégin, C., DesGranges, J.L., Guiot, J., Marion, J., Wicha, S., and Bégin, Y. 2014. Spatial analysis of the black spruce (*Picea mariana* (Mill) B.S.P.) radial growth response to climate in northern Quebec – Labrador Peninsula, Canada. Can. J. For. Res. **45**(3): 343–352. doi:10.1139/cjfr-2014-0080.

National Oceanic and Atmospheric Administration (NOAA). 2014. Teleconnections indices. Available from http://www.cpc.ncep.noaa.gov/products/precip/CWlink/daily_ao_index/teleconnections.shtml [accessed 10 October 2014].

Oksanen, J., Blanchet, F.G., Kindt, R., Legendre, P., Minchin, P.R., O'Hara, R.B., Simpson, G.L., Solymos, P., Stevens, M.H.H., and Wagner, H. 2015. vegan: community ecology package.

Plasse, C., Payette, S., and Matlack, G. 2015. Frost hollows of the boreal forest: a spatiotemporal perspective. J. Ecol. **103**(3): 669–678. doi:10.1111/1365-2745.12399.

Pothier, D., Margolis, H.A., Poliquin, J., and Waring, R.H. 1989. Relation between the permeability and the anatomy of jack pine sapwood with stand development. Can. J. For. Res. **19**(12): 1564–1570. doi:10.1139/x89-238.

Renwick, K.M., and Rocca, M.E. 2015. Temporal context affects the observed rate of climate-driven range shifts in tree species. Glob. Ecol. Biogeogr. **24**(1): 44–51. doi:10.1111/geb.12240.

Rossi, S., Deslauriers, A., Anfodillo, T., Morin, H., Saracino, A., Motta, R., and Borghetti, M. 2006. Conifers in cold environments synchronize maximum growth rate of tree-ring formation with day length. New Phytol. **170**(2): 301–310. doi:10.1111/j.1469-8137.2006.01660.x. PMID:16608455.

Schultz, J., Neuwirth, B., Winiger, M., and Löffler, J. 2009. Negative pointer years from Central European tree-rings caused by circulation patterns. TRACE, **7**: 78–84.

Schweingruber, F.H., Dieter, E., Serre-Bachet, F., and Bräker, O.U. 1990. Identification, presentation and interpretation of event years and pointer years in dendrochronology. Dendrochronologia, **8**: 9–38.

Sutinen, M.-L., Arora, R., Wisniewski, M., Ashworth, E., Strimbeck, R., and Palta, J. 2001. Mechanisms of frost survival and freeze-damage in nature. *In* Conifer cold hardiness. *Edited by* F. Bigras and S. Colombo. Springer Netherlands. pp. 89–120.

Visser, H., and Petersen, A.C. 2012. Inferences on weather extremes and weather-related disasters: a review of statistical methods. Clim. Past, **8**(1): 265–286. doi:10.5194/cp-8-265-2012.

Wang, Y., Hogg, E.H., Price, D.T., Edwards, J., and Williamson, T. 2014. Past and projected future changes in moisture conditions in the Canadian boreal forest. For. Chron. **90**(5): 678–691. doi:10.5558/tfc2014-134.

World Meteorological Organization (WMO). 2015. What is Climate? Available from http://www.wmo.int/pages/prog/wcp/ccl/faqs.php [accessed 24 August 2015].

Zang, C., and Biondi, F. 2013. Dendroclimatic calibration in R: the bootRes package for response and correlation function analysis. Dendrochronologia, **31**(1): 68–74. doi:10.1016/j.dendro.2012.08.001.

Zeppel, M.J.B., Wilks, J.V., and Lewis, J.D. 2014. Impacts of extreme precipitation and seasonal changes in precipitation on plants. Biogeosciences, **11**(11): 3083–3093. doi:10.5194/bg-11-3083-2014.